**Journal of Engineering and Sustainable Development**
Vol. 29, No. 06, November 2025
https://jeasd.uomustansiriyah.edu.iq/index.php/jeasd
ISSN 2520-0917
**Research Article**
https://doi.org/10.31272/jeasd.2627

# A Fractal-Based Compact Tunable Bandpass Filter with High Selectivity and Band Rejection

Areeg Fadhil Hussein[1*], Malik Jasim Farhan[2], Jawad K. Ali[3], Ameer B. Alsultani[4]

[1,2]Electrical Engineering Department, Mustansiriyah University, Baghdad, Iraq.
[3]Communication Engineering Department, University of Technology, Iraq.
[4]Department of Control Engineering and Information Technology, Budapest University of Technology and Economics, Faculty of Electrical Engineering and Information Technology, Budapest, Hungary.

*Email: areeg-fadhil@uomustansiriyah.edu.iq

**Article Info**

| | |
|---|---|
| **Received** | **27/04/2024** |
| **Revised** | **23/07/2025** |
| **Accepted** | **01/08/2025** |

**Abstract**

Fractal geometries have emerged as a promising approach for designing compact, tunable electronic components, particularly in microwave and radio-frequency circuits. This article presents a tunable filter for mobile communications that exploits a miniaturized open Ring Resonator, fabricated using the Minkowski fractal method. The fractal resulted in a 25.1% reduction in size, with an overall filter surface area of 51.84 $mm^2$. The proposed filter was constructed on a Roger RO4003 substrate with a center frequency of 2.69 GHz, a bandwidth of 0.14 GHz, and a compact size of 0.137λg × 0.13λg. This frequency will shift according to a variable capacitor added to the resonator with a range of 2.22-2.56GHz. The insertion loss of the tuning states ranged from 0.38 to 0.58 dB, the return loss was 20.7-28.4 dB, and the fractional bandwidth was 2.25-4.6%. This proposed design shows promising performance with 7.7 GHz band rejection, high selectivity, and a compact size.

**Keywords:** Bandpass filter, Fractal filter, Microstrip filter, Tunable filter.

## 1. Introduction

Microwave filters have become essential to communications systems at both the front and the end [1]. Filters are important when a specific frequency band is required, with high rejection of undesired signals [2]. There are many parameters to consider when designing and implementing microwave filters, such as selectivity, bandwidth, size, cost, insertion loss, and reliability [3].

Current communication systems operate in diverse frequency bands to align with modern trends. Tunable filters are the best solution for providing flexibility in such systems. Tuning enables adjustments to meet specific requirements in various applications, such as telecommunications, radar systems, and wireless communication [4], [5].

Plentiful research and structures presented for microstrip tunable bandpass filters like stub-loaded resonators (SLR), step impedance resonators (SIR) [6], and ring resonators with different tuning techniques such as varactors, PIN diodes, variable capacitance, or stretching materials [7].

In [8], an Nth-order filter was designed by cascading resonators in parallel and tuning them using varactors controlled by their biasing voltage. Li et al. [9] have proposed a tri-band BPF that operates through a standard feed line, with varactors as tuning and switching elements controlled by varying their voltages; tuneability and switchability have been achieved. Furthermore, it is possible to control each passband individually. A tunable filter with applied stress to the substrate of the microstrip Chebyshev band pass filter has been proposed by Luo [10]. The results showed that the filter's characteristics remained the same, except that the frequency and the ripple values changed.

On the other hand, Iqbal et al. [11] have presented a filter consisting of four poles constructed by utilizing two poles and optimizing the cavity in the Substrate Integrated Waveguide SIW. Both designs used a varactor diode to provide tunability to the filters. Wan et al. [12] have presented the design of a resonator with multiple layers of a folded configuration and a substrate-integrated defected ground structure (SIDGS). This resonator has been designed to generate a bandpass filter (BPF) with two particular frequency bands that may be shifted independently. Roy et al. [13] developed an algorithm to create artificial neural network (ANN) models for forecasting appropriate tuning parameters for adjustable bandpass filters. The lumped-element circuit model and Electromagnetic EM



Work of This Research is Licensed under CC BY

model of bandpass filters, which aid in constructing tunable filters, are used to validate the method.

Minkowski fractals were used by Ali [14] to design a compact single-band, dual-mode resonator with a 72% size reduction. In [15], an 88% size reduction was achieved using a dual-mode resonator based on a modified Minkowski fractal geometry; however, the use of fractal iterations is limited by the filter response. In [16], ring resonators based on modified Minkowski fractal geometry were used as a miniaturized triple-band stop filter. Fractal geometry is individualized by self-assembling and inhabiting space in a successful miniaturizing way [17].

Although many tunable bandpass filter designs have been reported using techniques such as step impedance resonators (SIR), stub-loaded resonators (SLR), and varactor-based tuning, most existing structures suffer from large physical size, limited tunability range, and low selectivity. Moreover, several previous studies achieved compactness through fractal geometries but did not combine fractal miniaturization with defected ground structures (DGS) to improve rejection and tuning precision.

To address these limitations, this study aims to design and simulate a Minkowski fractal-based adjustable bandpass filter for use across various fields, including 4G LTE mobile communication, satellite communication, Wi-Fi, and Bluetooth. A defected ground structure (DGS) was incorporated to improve the filter's ability to pass some frequencies and reject others selectively.

The novelty of this research lies in the combined use of Minkowski fractal geometry and a defected ground structure (DGS) to design a compact, highly selective, tunable bandpass filter. This configuration enables significant miniaturization while maintaining superior transmission characteristics.

The main contributions of this work are the development of a tunable Minkowski fractal-based bandpass filter optimized for the 2.22–2.56 GHz range, with excellent selectivity and suppression.

## 2. Method of the research

The proposed bandpass filter in Fig.1 is designed to tune with a range of (2.22-2.56 GHz), which is used in mobile communication, Wi-Fi, Bluetooth, etc [18]. The filter's center frequency is 2.65 GHz with band rejection up to 7.77 GHz, a bandwidth of 0.14 GHz, a fractional bandwidth of 5.2%, an Insertion Loss (IL) of 0.41 dB, and a Return Loss (RL) of 25.68 dB. The substrate used in this design is Rogers RO4003, with a dielectric constant of 3.55 and a loss tangent of 0.0027, and a thickness of 0.508 mm. Fig. 2 shows a flowchart that elaborates on the filter design.

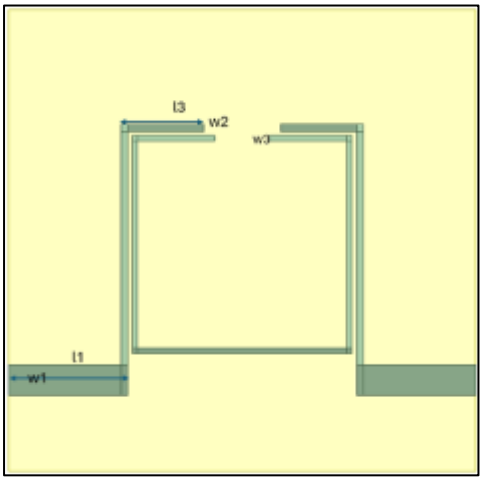


(a)

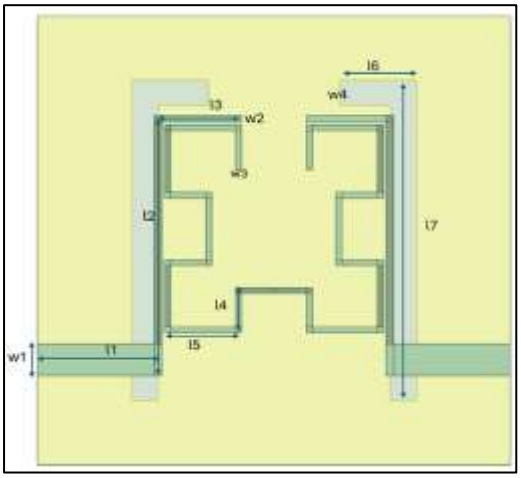


(b)

**Figure 1.** a) Zero iteration filter. b) filter layout with DGS.

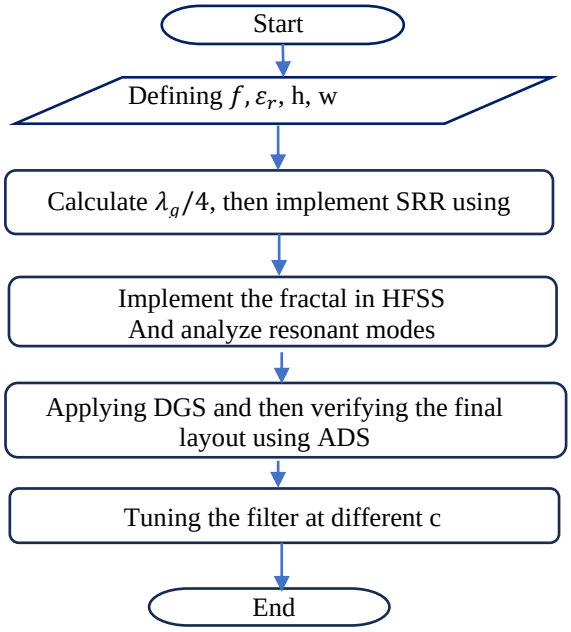


**Figure 2.** Design procedure flowchart.

### 2.1. Design Procedure

This section describes the steps of designing the proposed filter from scratch. The length of the open ring resonator in Fig.1(a) is determined using the following [3]

$$\lambda_g = \frac{300}{f(GHz)\sqrt{\varepsilon_{re}}} \quad (1)$$

$$\varepsilon_{re} = \frac{\varepsilon_r+1}{2} + \frac{\varepsilon_r-1}{2}\left\{\left(1+12\frac{h}{w}\right)^{-0.5} + 0.04\left(1-\frac{w}{h}\right)^2\right\} \quad (2)$$

Where $\lambda_g$ is the guided wavelength at a center frequency of 2.65 GHz, h is the thickness of the substrate of 0.508 mm, $\varepsilon_r$ is the dielectric constant of 3.55, and w is the conductor width of 0.2 mm—applying the first iteration of Minkowski fractal to miniaturize the filter size [14], where the center frequency has been changed to 2.77 GHz.

After implementing the Minkowski fractal onto the filter, the surface area of the open ring resonator decreased from 69.2 $mm^2$ to 51.84 $mm^2$, resulting in an overall reduction of 25.1%. The resonance modes of the Minkowski resonator are revealed by plotting the current field distribution at the unwanted modes, which indicate the areas of the resonator that induce these modes, as seen in Fig. 3. Then, they can be eliminated using a defected ground structure. DGS offers an improved approach to achieving a rejection band within a specific frequency range in periodic and nonperiodic arrays [19].

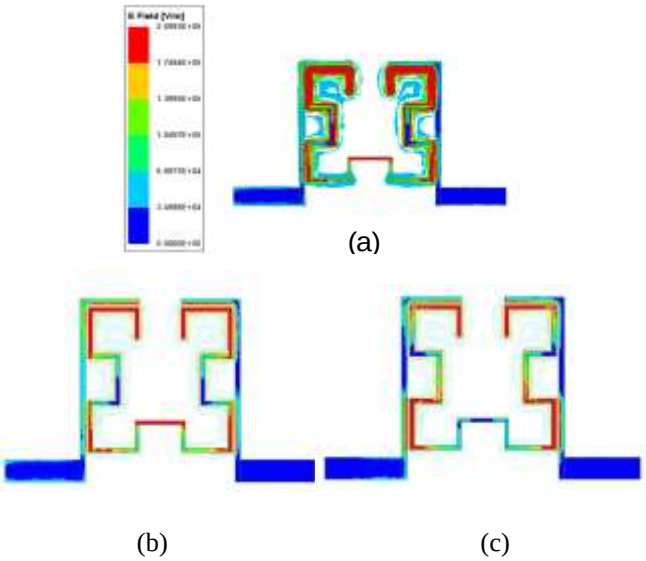

(a) (b) (c)

**Figure 3.** Resonant modes: a) first mode at 2.77GHz. b) second mode at 5.25GHz. c) third mode at 8.06GHz.

Fig. 4 shows the S11 results for the three approaches, and Fig. 5 shows the S21 results.

Fig. 1(b) and Fig. 6 show the final structure of the bandpass filter and its response, with the dimensions illustrated in Table 1. The center frequency of 2.69 GHz, insertion loss (IL) of 0.41 dB, return loss (RL) of 30.42dB, bandwidth of 140MHz with band selectivity transmission zero TZ at -40 dB, and band rejection up to 7.9 GHz.

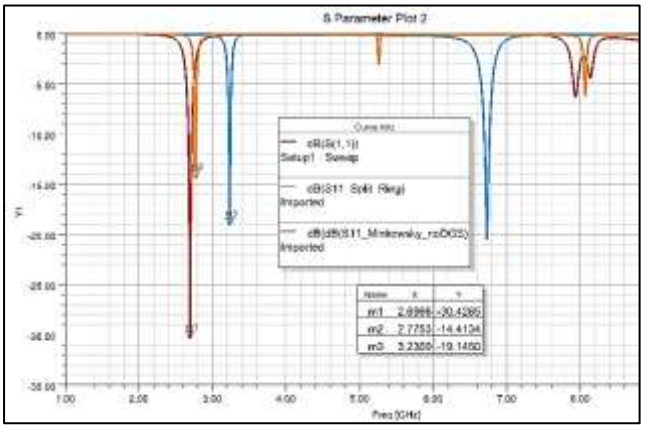


**Figure 4.** S11 comparison of the design progress.

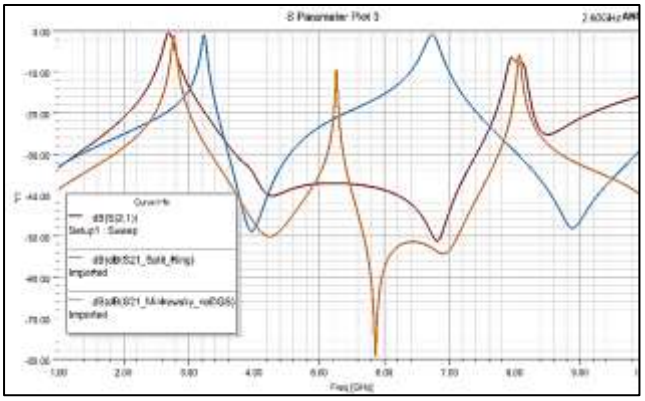


**Figure 5.** S21 comparison of the design progress.

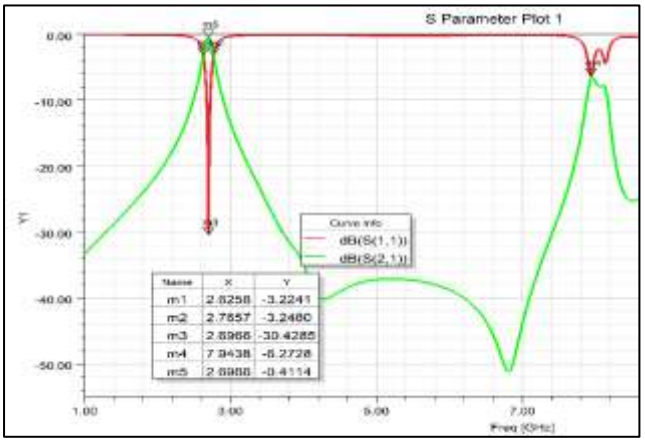


**Figure 6.** S-parameters of the final structure in HFSS.

**Table 1.** Physical dimensions of the filter (mm).

| 11 | 12 | 13 | 14 | w1 | w2 | 15 | 16 |
|---|---|---|---|---|---|---|---|
| 4.14 | 9.28 | 2.95 | 1.6 | 1.13 | 0.25 | 2.6 | 2.6 |
| **17** | **w3** | **s1** | **w4** | **$\varepsilon_r$** | **h** | **Tangent loss** | |
| 11.4 | 0.2 | 0.12 | 0.9 | 3.55 | 0.508 | 0.0022 | |

To validate the outcomes of the final filter design, we utilized the ADS EM simulator to simulate the final filter layout. The resulting response, along with the ADS layout, is presented in Figs. 7 and 8.

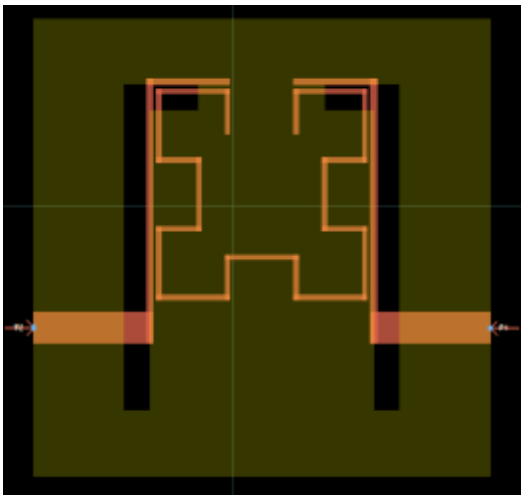

**Figure 7.** The final layout in ADS.

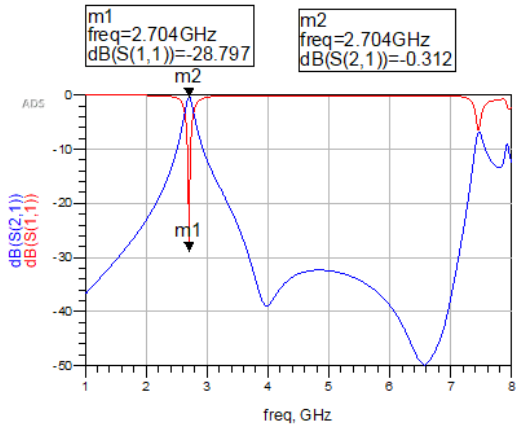


**Figure 8.** S-parameters of the final structure in ADS.

### 2.2. Tuning Circuit

Fig. 9 demonstrates the tuning of the variable capacitance (C) from 0.01 pF to 0.09 pF using HFSS simulation. The capacitance is placed in the filter's gap. The C values have been determined by calculating the coupling matrix and the $g_k$ values using the formulas in [20]. $\boldsymbol{g_0 = 1}$, $\boldsymbol{g_2 = 0.201008}$, $\boldsymbol{g_3 = 1}$, Coupling matrix= $[\mathbf{4.974937} \quad \mathbf{4.974937}]$.

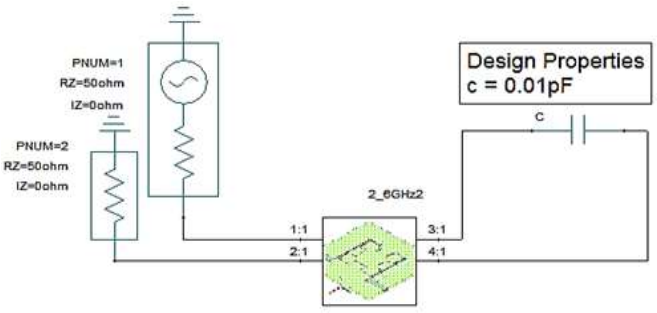


**Figure 9.** Tuning circuit in HFSS.

### 3. Results and Discussion

In this paper, a bandpass filter has been designed using Rogers RO4003, with a dielectric constant of 3.55 and a loss tangent of 0.0027, and a substrate thickness of 0.508 mm. The conductor width is 0.2 mm. The center frequency of 2.69 GHz, insertion loss (IL) of 0.41 dB, return loss (RL) of 30.42 dB, bandwidth of 140 MHz, with band selectivity transmission zero TZ at -40 dB, and band rejection up to 7.9 GHz using HFSS EM simulator.

The S11 and S21 variations through the tuning process are spotted in Fig.10 and Fig.11. The filter was tuned using variable capacitance with C=0.01 pF; The center frequency has been changed to 2.56 GHz with IL=0.38 dB, RL=28.49 dB, BW=0.12 GHz, fractional bandwidth=4.6%, and the selectivity TZ at 48.78 dB.

When C=0.03 pF, the center frequency has been changed to 2.45 GHz with IL=0.4 dB,

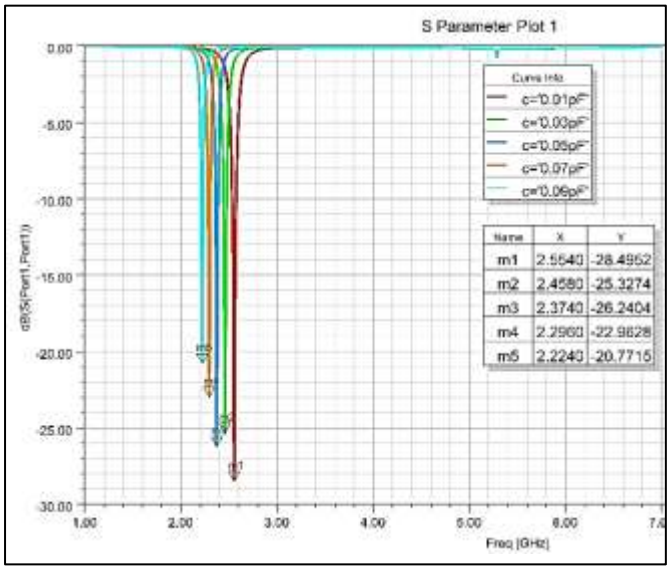


**Figure 10.** S11 Tunning circuit results.

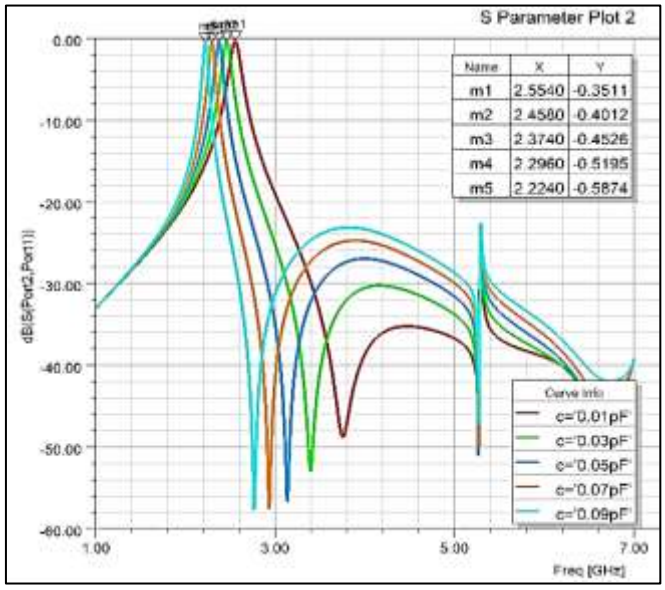


**Figure 11.** S21 Tunning circuit results.

RL= 25.32 dB, BW=0.09 GHz, fractional bandwidth=3.6%, and the selectivity TZ=52.66 dB. At C=0.05 pF, the center frequency has been changed to 2.37 GHz with IL=0.45 dB, RL=26.24 dB, BW=0.08 GHz, fractional bandwidth=3.3%, and the selectivity TZ=56.7 dB.

At C=0.07 pF, the center frequency has been changed to 2.29 GHz with IL=0.51 dB, RL=22.96 dB, BW=0.06 GHz, fractional bandwidth=2.6%, and the selectivity TZ=57.56 dB. At C=0.09 pF, the center frequency has been changed to 2.22 GHz, with IL=0.58 dB, RL=20.77 dB, BW=0.05 GHz, fractional bandwidth=2.25%, and selectivity TZ=57 dB. In all cases, the band rejection remains constant at 7 GHz.

Compared with similar tunable bandpass filters [1]-[3], the proposed fractal filter achieves approximately 25% size reduction and at least 1 GHz of wider band rejection, with improved insertion and return loss performance, as shown in Table 2.

**Table 2.** Comparison with previous works.

| **Ref.** | [1] | [2] | [3] | **Prop.** |
|---|---|---|---|---|
| Tuning range (GHz) | 1.53-2.318 | 3.15-6.15 | 2.4-3.4 | 2.22-2.56 |
| BW(GHz) | 1-0.455 | 0.6-1.6 | N.M. | 0.05-0.14 |
| Band rejection | ≈ 3.5 | ≈ 6 | ≈ 6 | > 7 |
| RL (dB) | 14-25.44 | N.M. | N.M. | 22.96 -28.49 |
| IL (dB) | 1.5-0.852 | 2 | 1< | 0.58-0.38 |
| Size $\lambda_g \times \lambda_g$ | 0.33X 0.498 | 0.258X 0.255 | 0.326X 0.218 | 0.137X0.13 |

The proposed filter offers high-band rejection, improved insertion and return loss, and a compact size, making it an effective and efficient option compared to previous work. However, it has a narrower tuning range and capacity. This makes it suitable for applications requiring high precision and a compact size, but it might limit its flexibility across a broader frequency range.

The electromagnetic simulation results confirm that the proposed Minkowski fractal-based bandpass filter achieves superior selectivity, rejection, and compactness. The S-parameter comparison shows sharp attenuation outside the passband, with low insertion loss and stable return loss over the 2.22–2.56 GHz tuning range.

The introduction of the Minkowski fractal iteration significantly improves the filter's characteristics. As the iteration order increases, the resonator path length becomes longer while occupying the same projected area. This geometric modification effectively increases the distributed capacitance and inductance, thereby lowering the resonant frequency and improving impedance matching in the desired passband. Consequently, the first-order fractal iteration resulted in a 25.1% size reduction and produced a sharper roll-off rate, reflected in higher transmission zeros (TZs) exceeding –57 dB.

However, increasing the number of fractal iterations introduces additional discontinuities and electromagnetic coupling segments, potentially narrowing the adequate bandwidth due to greater energy confinement within the resonator structure. Therefore, there is a trade-off between miniaturization and bandwidth preservation: higher fractal complexity enhances selectivity but slightly decreases the fractional bandwidth. In this design, the chosen single-iteration Minkowski fractal achieves an optimal balance, maintaining a fractional bandwidth of 2.25%-4.6% while significantly improving selectivity compared with conventional ring resonators.

The defective ground structure (DGS) further enhances selectivity by introducing additional transmission zeros and suppressing spurious modes, thereby maintaining a stable rejection band above 7 GHz. The combined effect of the fractal iteration and DGS yields a compact, high-performance filter with IL = 0.38–0.58 dB and RL = 20.7–28.4 dB.

Although this study focuses on simulation-based validation, future work will include fabrication and experimental measurements using a photolithographic process on a Rogers RO4003 substrate. Scattering-parameter measurements with a vector network analyzer (VNA) will be conducted to verify the simulated results and evaluate environmental stability and tunability under practical biasing conditions. Such experimental verification will provide further confirmation of the proposed filter’s applicability for 4G/5G and Wi-Fi front-end modules.

## 4. Conclusions

This paper presented a Minkowski fractal bandpass filter with high selectivity and band suppression at a center frequency of 2.69 GHz with an insertion loss of 0.41 dB and a return loss of 40 dB. The filter was implemented using HFSS, and its result

was verified using an ADS simulation kit. Afterward, the final filter layout was tuned with variable capacitance using an HFSS simulation circuit. A tuning range of 2.22 GHz - 2.56 GHz was achieved with fractional bandwidths of 2.25% - 4.6%. The band suppression is 57 dB – 40 dB. Further, the size can be miniaturized through additional iterations.

The main contributions of the proposed Minkowski fractal bandpass filter are the demonstration of a 25.1% reduction in physical size compared to the conventional ring-resonator filter while maintaining broad-band rejection exceeding 7 GHz, and the integration of a defected ground structure to eliminate unwanted resonant modes and improve out-of-band rejection. In addition, validation of the proposed design using HFSS and ADS electromagnetic simulations shows low insertion loss (0.38–0.58 dB) and high return loss (20–28 dB).

## Acknowledgments

The authors would like to thank Mustansiriyah University (www.uomustansiriyah.edu.iq), Baghdad, Iraq, for its support in the present work.

## Conflict of interest

The authors declare that there are no conflicts of interest regarding the publication of this manuscript.

## Author Contribution Statement

Areeg F. Hussein developed the theory, performed the computations, and verified the analytical methods. Malik J. Farhan and Jawad K. Ali proposed the research problem and supervised the work. All authors discussed the results and contributed to the final manuscript.

## References

[1] H. I. Khani and A. S. Ezzulddin, "A survey on microstrip single/multiband bandpass filter for 5G applications," *Engineering and Technology Journal*, vol. 41, no. 2, pp. 1–17, Jan. 2023, doi: https://doi.org/10.30684/etj.2022.135858.1288.

[2] I. Hunter, *Theory and Design of Microwave Filters*. London, UK: The Institution of Engineering and Technology, 2001.

[3] J. Hong and M. J. Lancaster, *Microstrip Filters for RF/Microwave Applications*. New York, NY, USA: Wiley, 2001, doi: https://doi.org/10.1002/0471221619.

[4] S. L. Tripathi, P. A. Alvi, and U. Subramaniam, Eds., *Electrical and Electronic Devices, Circuits, and Materials*. Hoboken, NJ, USA: Wiley, 2021, doi: https://doi.org/10.1002/9781119755104.

[5] M. Qin et al., "Varactor-based continuously tunable microstrip bandpass filters: A review, issues and future trends," *IEEE Access*, vol. 12, pp. 57443–57457, 2024, doi: https://doi.org/10.1109/ACCESS.2024.3383788.

[6] A. J. Alazemi, "Dual-band and wideband bandpass filters using coupled lines and tri-stepped impedance stubs," *Micromachines*, vol. 14, no. 6, Jun. 2023, doi: https://doi.org/10.3390/mi14061254.

[7] V. A. Karpova and N. V. Ivanov, "Optimization of a microstrip tunable bandpass filter design," in *Proc. 2021 IEEE Conf. Russian Young Researchers in Electrical and Electronic Engineering (ElConRus)*, Jan. 2021, pp. 129–132, doi: https://doi.org/10.1109/ElConRus51938.2021.9396434.

[8] Q. Xiang et al., "A 5th-order constant bandwidth tunable bandpass filter with two cascaded trisection structures," *IEEE Trans. Circuits Syst. II, Exp. Briefs*, vol. 70, no. 1, pp. 126–130, Jan. 2023, doi: https://doi.org/10.1109/TCSII.2022.3208601.

[9] Z. Li et al., "Compact dual-/tri-/quad-band bandpass filters with independently frequency-tunable and switchable passbands," *Int. J. Microw. Wireless Technol.*, vol. 13, no. 4, pp. 322–334, May 2021, doi: https://doi.org/10.1017/S1759078720001130.

[10] X. Luo et al., "Design of a stretchable Chebyshev microstrip gap coupled band-pass filter," in *Proc. 2021 Int. Conf. Microwave and Millimeter Wave Technology (ICMMT)*, 2021, doi: https://doi.org/10.1109/ICMMT52847.2021.9618223.

[11] A. Iqbal et al., "Tunable SIW bandpass filters with improved upper stopband performance," *IEEE Trans. Circuits Syst. II, Exp. Briefs*, vol. 67, no. 7, pp. 1194–1198, Jul. 2020, doi: https://doi.org/10.1109/TCSII.2019.2936495.

[12] Y. Wan et al., "Independently tunable compact dual-band bandpass filter with high selectivity and wide stopband using multilayer folded dual-mode SIDGS resonator," in *IEEE MTT-S Int. Microw. Symp. Dig.*, 2023, pp. 827–830, doi: https://doi.org/10.1109/IMS37964.2023.10187986.

[13] C. Roy, P. Zhao, and K. Wu, "ANN model development for tunable bandpass filter," in *Proc. 2021 51st Eur. Microw. Conf. (EuMC)*, Apr. 2022, pp. 297–300, doi: https://doi.org/10.23919/EuMC50147.2022.9784306.

[14] J. K. Ali, "A new miniaturized fractal bandpass filter based on dual-mode microstrip square ring resonator," in *Proc. 5th Int. Multi-Conf. Syst., Signals Devices (SSD)*, 2008, doi: https://doi.org/10.1109/SSD.2008.4632887.

[15] J. K. Ali and N. N. Hussain, "An Extra Reduced Size Dual-Mode Bandpass Filter For Wireless Communication Systems," 2011, doi: https://doi.org/10.13140/2.1.2279.7767.

[16] H. S. Ahmed et al., "A compact triple band BSF design based on Minkowski fractal geometry," in *Proc. 2016 18th Mediterr. Electrotech. Conf. (MELECON)*, Apr. 2016, pp. 1–5, doi: https://doi.org/10.1109/MELCON.2016.7495453.

[17] E. Arzt, H. Quan, R. M. McMeeking, and R. Hensel, "Functional Surface Microstructures Inspired by Nature – from Adhesion and Wetting Principles to Sustainable New Devices," Progress in Materials Science, vol. 120, p. 100823, Jul. 2021, doi: https://doi.org/10.1016/j.pmatsci.2021.100823 .

[18] A. Gupta and R. K. Jha, "A survey of 5G network: Architecture and emerging technologies," *IEEE Access*, vol. 3, pp. 1206–1232, 2015, doi: https://doi.org/10.1109/ACCESS.2015.2461602.

[19] A. Basheer et al., "Design of bandpass filter for 5G applications with high-selectivity and wide band rejection," in *Proc. Al-Muthanna 2nd Int. Conf. Eng. Sci. Technol. (MICEST)*, 2022, pp. 179–183, doi: https://doi.org/10.1109/MICEST54286.2022.9790185.

[20] R. J. Cameron, C. M. Kudsia, and R. R. Mansour, *Microwave Filters for Communication Systems*. Hoboken, NJ, USA: Wiley, 2018, doi: https://doi.org/10.1002/9781119292371.

[21] A. A. Al-Mudhafar, N. Al-Khafaji, and H. J. Al-Battat, "Split ring resonators SRRs based bandwidth and center frequency tunable bandpass filter," *AIP Conf. Proc.*, vol. 2293, 2020, p. 040011, doi: https://doi.org/10.1063/5.0027381.

[22] A. Golestanifar, G. Karimi, and A. Lalbakhsh, "Varactor-tuned wideband band-pass filter for 5G NR frequency bands n77, n79, and 5G Wi-Fi," *Sci. Rep.*, vol. 12, no. 1, p. 16330, Sep. 2022, doi: https://doi.org/10.1038/s41598-022-20593-x.

[23] A. Sondas, "Tunable band-pass microstrip filter design based on split-ring element," *Wirel. Pers. Commun.*, vol. 132, no. 4, pp. 2283–2292, Oct. 2023, doi: https://doi.org/10.1007/s11277-023-10233-6.